

	Experiment title: Full-field XANES study Chinese Ming blue and white porcelain-chromogenic mechanisms	Experiment number: HG44
Beamline: ID21	Date of experiment: from: 28/08/2014 to: 30/08/2014	Date of report: <i>Received at ESRF:</i>
Shifts: 6	Local contact(s): FAYARD Barbara	
Names and affiliations of applicants (* indicates experimentalists): Marine Cotte * (ESRF, Grenoble) Zeyang Feng (Archaeometry Lab, Laboratory Sun Yat-sen University, China) Emeline Pouyet * (ESRF, Grenoble) Phillipe Sciau * (CEMES-CNRS, Toulouse) Tiequan Zhu (Archaeometry Lab, Laboratory Sun Yat-sen University, China) Tian Wang (CEMES-CNRS, Toulouse)		

Report:

NB: Originally, we requested 15 shifts and the comments made by the Review Committee was “*Interesting proposal but not enough beamtime available at ID21*”. Ultimately, the proposal was promoted from the reserve list and we got 6 shifts in August we used to study 4 typical shreds of Qinghua porcelain produced during Ming Dynasty shown in Fig. 1. Not only the feasibility was validated over concentrated pigment regions, but also significant results were obtained and a paper is in preparation to be submitted to Analytical Chemistry.

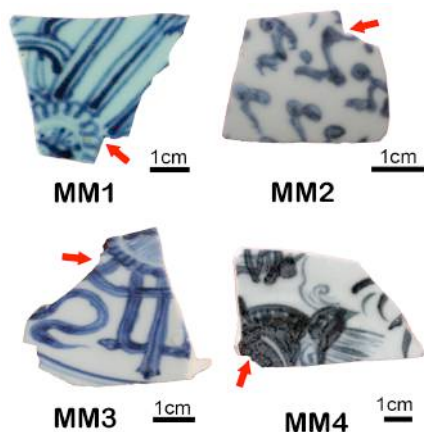


Fig. 1 Photos of the four studied sherds. The sampling zones are indicated with red arrows.

Full-field recordings were performed on thin cross section samples previously prepared at CEMES. The preparation method was similar to the one used for the study of Roman potteries [F. Meirer 2013]. The main steps are summarized in figure 2. After several cutting steps (1-3) in order to obtain two strips with blue decors (4), the strips were glued together glaze against glaze to form a sandwich (5). Subsequently, the sandwich was cut into several $\sim 500 \mu\text{m}$ slices and then each one was embraced with glue and placed on a glass slide (6). Slices were temporarily mounted on a movable support in brass with a dental wax (7). After polishing the first face, the movable support was heated in order to melt the wax. The sample was flipped and glued with wax. A copper grid (used

as reference for the thickness) was added on the support, glued with wax as well. The slice was polished down to have the same thickness with the copper grid (40-60 μm). Finally, a copper washer (8) was glued to the final thin-section for safeguarding the samples and facilitating their transport (9) and installation on ESRF sample-holder (10). The different thin lamellas obtained from the same sample were noticed with adding -Cn (n lamella number) to the specimen number.

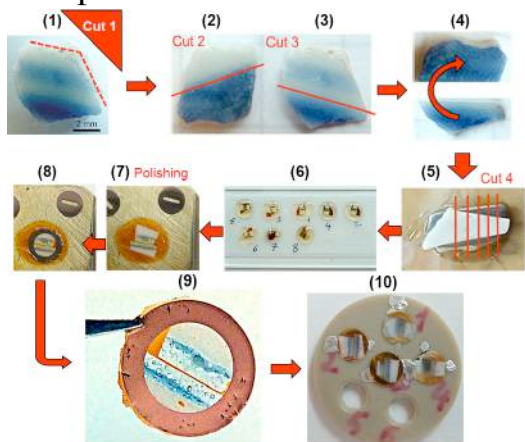


Fig. 2 Main steps of the cross-section preparation: from the fragment sampling (1) to the thin cross-section lamella (9) placed on the specific ID21 sample holder (10).

The first 0.5 shift was used to configurate the beamline in full-field mode at Fe K-edge to Co K-edge. The other 5.5 shifts was used to record full-field XANES stacks. The energy of incident X-ray beam is tuned over the Co K-edge for all four samples (208 different energies, from 7670.2 to 7910.1 eV, with energy steps from 0.3 to 2.2 eV depending on the energy domain) and over the Fe K-edge for two samples (213 different energies, from 7060.0 to 7302.1 eV, with energy steps from 0.3 to 2.2 eV). A 20x optical objective is used to magnify the image onto a CMOS PCO. edge camera, giving a pixel size of $0.32 \times 0.32 \mu\text{m}^2$. After data pre-processing (flat field correction and image alignment), the FF-XANES stack consisting of a series of normalized images was built using PyMca software.

Then the data processing (including PCA and k-means clustering) were performed using the freely available software package TXM-Wizard [Y. J. Liu 2012]. In addition, SR- μ XRF mappings were carried out using the Scanning X-ray Microscope at ID21 on the same samples thanks to in-house beamtime (not presented here). One of XRF images is shown on the ESRF “beauty of science” page (<http://www.esrf.eu/home/news/beauty-of-science/content-news/beauty-of-science/beauty-Qinghua-procelain.html>).

Full-field XANES analyses at the Co K-edge

The results obtained for the MM2-C3 sample are shown in Fig. 3. The transmission image recorded at 7670 eV, below the Co K-edge, revealed the presence of several large bubbles-

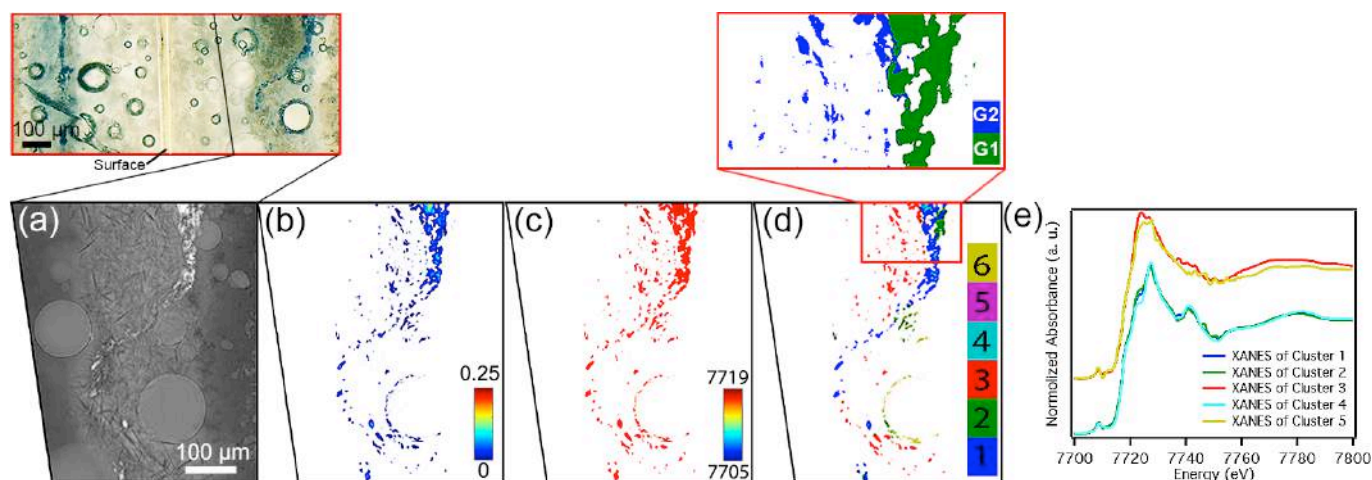


Fig. 3 Results of FF-XANES analyses performed at the Co K-edge (corresponds to the area of Co fluorescence intensity map shown on the upper left map) for MM2-C3 with: (a) the transmission image of sample thin-section recorded at 7670 eV; (b) and (c) The edge jump map (correlated to Co concentration) and the edge energy map (correlated to Co valence). The scale bar for the edge jump map and for the edge energy reports the values of the (absorption) edge jump and the energy of the (absorption) edge in eV, respectively; (d) and (e) The image segmentation of the corresponding zone based on PCA and k-means clustering and the corresponding average XANES of each cluster. The color bar for image segmentation is in agreement with the spectra of pertinent clusters. Cluster 1, 2 and 4 are grouped as G1 and cluster 3 and 6 are grouped as G2 as shown in the zooming image

pores (diameter of $\sim 100 \mu\text{m}$ or smaller) and a multitude of long narrow strips in the pigment zone attributed to anorthite crystals (Fig. 3a). The edge jump map (Fig. 3b) shows a distribution of the Co map, which is more concentrated in the pigment zone while quiet limit up to the surface. The edge energy map (Fig. 3c) obtained from pixels with a signal to noise (SNR) level superior to 0.014 shows no significant spectral features variation, with a edge energy at $\sim 7717 \text{ keV}$, consistent with bivalent cobalt [C. Maurizio 2010; Figueiredo 2012]. PCA approach and subsequent k-means clustering were processed for a closer inspection. The first three principal components were considered to cover the cardinal significant information, clustered into $k = 6$ groups. The corresponding XANES spectra can be divided into two groups according their similarities: cluster 1, 2 and 4 and cluster 3 and 6 were grouped as G1 and G2 respectively (Fig. 3e). Cluster 5 was not taken into account due to a low SNR value. With a white line at $\sim 7726 \text{ eV}$, the spectra of G1 are congruent with the ones of of aluminate (CoAl_2O_4) particles in which Co^{2+} ions are in tetrahedral coordination [C. Maurizio 2010; M. O. Figueiredo 2012]. Compared to these spectra, the XANES spectra of G2 exhibit the same pre-edge and the same rising edge, also indicating a dominant bivalent state for the cobalt ions. However, the energy crests and the white line are clearly different, which the latter is broader and moves to lower energy ($\sim 7724 \text{ eV}$). Therefore, from the distributions of the two groups illustrated in the zooming image segmentation (Fig. 3d), the diffusions of cobalt aluminate particles and bivalent Co in a glassy matrix are presented clearly.

A second sample of the same specimen (MM2-C1) was analyzed the same way (Fig. 4). The results are similar but the higher Co content outside the particles results in a higher SNR, which allows including increasing pixels numbers in the PCA processing. The differences between the spectral features in the particles and in the glassy matrix are clearer: the cluster 1 and 2 showed the similar traits with group 1 and 2 (Fig. 3), corresponding to the cobalt aluminate particles and bivalent Co in glassy matrix, respectively. Thus, the distributions of both clusters accurately portray the distributions of particles and Co ions in the glassy matrix.

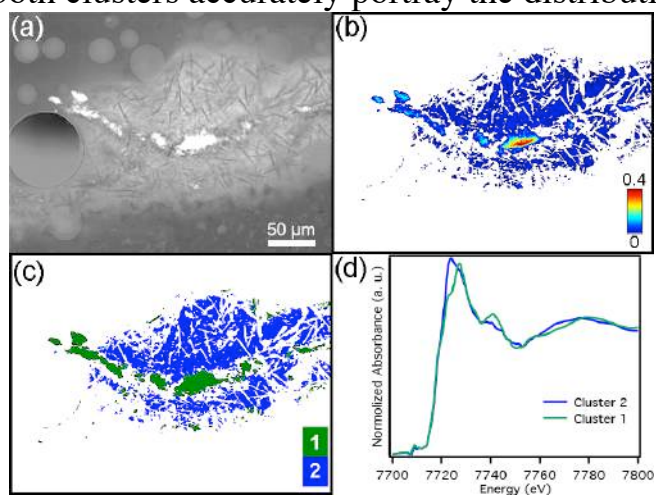


Fig. 4 Results of FF-XANES analysis across the Co K-edge for MM2-C1: (a) the transmission image recorded at 7670 eV, (b) the edge jump map, (c) the image segmentation based on PCA and k-means clustering and (d) the corresponding average XANES for cluster 1 and 2.

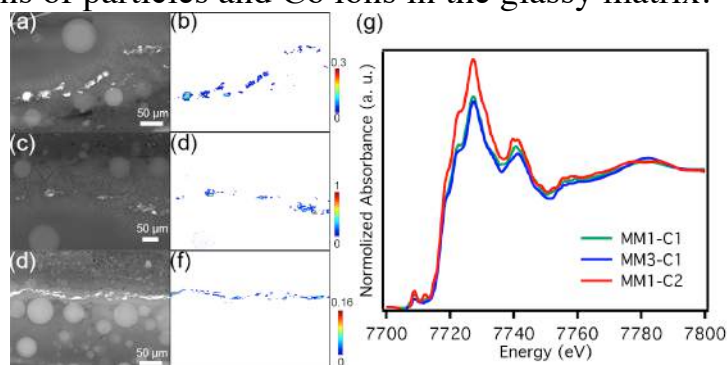


Fig. 5 Results of FF-XANES analysis performed at the Co K-Edge. The transmission image was recorded at 7670 eV from top to bottom for MM1-C1, MM1-C2, MM3-C1, as shown in (a), (c) and (d), respectively. Image (b), (d) and (f) presents respectively the edge jump map of each sample. The average XANES of each cluster was also displayed in (g).

MM1-C1, MM1-C2 and MM3-C1 exhibit similar results with high Co concentrated zone corresponding to cobalt aluminate particles (Fig. 5). In contrast, no based Co particles were detected in MM4-C2 in agreement with SR-XRF investigation (not presented here but), which revealed a quite homogeneous distribution of Co.

Full-field XANES analyses at the Fe K-edge

Two samples were also analyzed by FF-XANES across the Fe K-edge (Fig. 6). For MM1-C2, the edge jump map reveals a rather homogeneous distribution around the long narrow strips (anorthite crystals) and the cobalt aluminate particles. There is no variance of the edge energy (~ 7712.1 eV) and the PCA approach confirms that there is only one type of XANES spectrum. The spectrum is very close to the one of bivalent iron dispersed in a glassy matrix [G. Giuli 2003; A. J. Berry 2003]. The Fe-rich thin layer present on the surface of the glaze was not included in the FOV, which was focusing on Co particles. By contrast to MM1-C2, the edge jump map of MM4-C2 indicates a more homogeneous distribution of Fe, consistent with XRF scanning measurements. The PCA approach also revealed only one type of XANES spectra but the edge energy is slightly higher which can be an indicator of the presence of a small amount of trivalent iron.

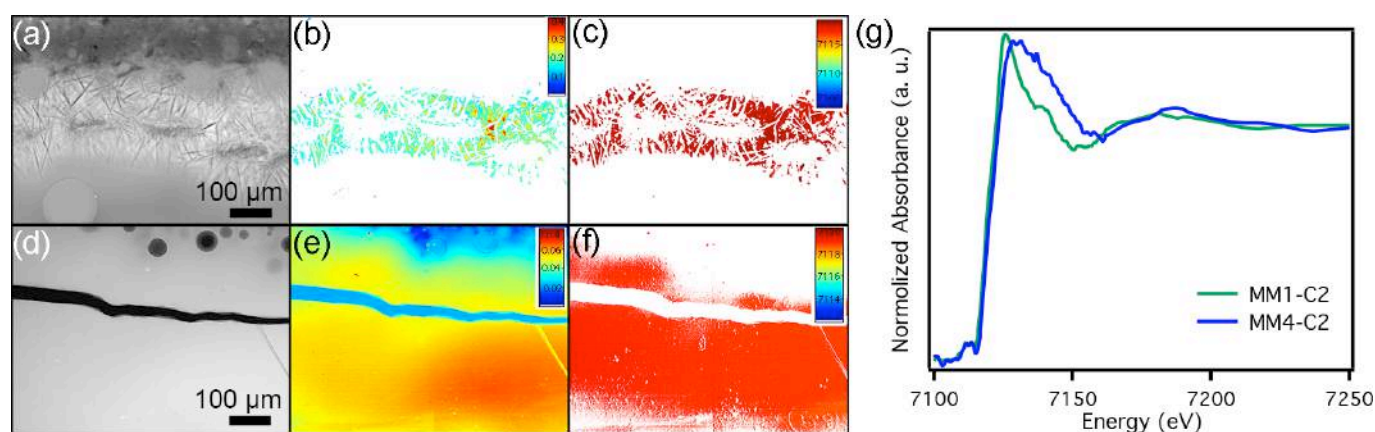


Fig. 6 Results of FF-XANES analysis of MM1-C2 and MM4-C2 across the Fe K-edge (from top to bottom). The transmission image recorded at 7050 eV shown as (a) and (d), respectively. Based on the XANES evaluation, (b) and (e) presents respectively the edge jump map calculated (correlated to Fe concentration) and (c) and (f) manifested respectively the edge energy map calculated (correlated to Fe valence). The scale bar for the edge jump map and for the edge energy reports the values of the (absorption) edge jump and the energy of the (absorption) edge in eV, respectively. The corresponding average XANES of whole bulk was displayed for each sample (g).

In conclusion, these investigations revealed the micro-composition of the blue decors for the first time. XANES spectra showed that Co is present under two chemical forms: CoAl_2O_4 in the pigment particles, and Co ions in the glassy matrix. The results show that the oxidation state, chemical environment, concentration and distribution of cobalt-based pigment play a key role in the hue variances of blue decors. The distribution and concentration of Co ions in glaze affect the blue color intensity, with higher concentration and diffusion of Co ions leading to a bluish glaze in some Qinghua porcelains.

References

- A. J. Berry, H. C. O'Neill, K. D. Jayasuriya, S. A. J. Campbell and G. J. Foran, *American Mineralogist*, 2003, 88, 967–977
- F. Meirer, Y. Liu, E. Pouyet, B. Fayard, M. Cotte, C. Sanchez, J. C. Andrews, A. Mehta and P. Sciau, *J. Anal. Atomic Spectro.*, 2013, 28, 1870–1883.
- Y. J. Liu, F. Meirer, P. A. Williams, J. Y. Wang, J. C. Andrews and P. Pianetta, *J. Synchrotron Radiat.*, 2012, 19, 281–287.
- C. Maurizio, N. E. Habra, G. Rossetto, M. Merlini, E. Cattaruzza, L. Pandolfo and M. Casarin, *Chem. Mater.* 2010, 22, 1933–1942.
- M. O. Figueiredo, T.P. Silva, J.P. Veiga, *Journal of Electron Spectroscopy and Related Phenomena*, 2012, 185, 97–102.
- G. Giuli, E. Paris, G. Pratesi, C. Koeberl and C. CIPRIANI, *Meteoritics & Planetary Science*, 2003, 38, 1181–1186.